The Interaction of the Human GGA1 GAT Domain with Rabaptin-5 Is Mediated by Residues on Its Three-Helix Bundle†

Peng Zhai,‡ Xiangyuan He,§ Jian Liu,|| Nancy Wakeham,‡ Guangyu Zhu,‡ Guangpu Li,|| Jordan Tang,§,|| and Xuejun C. Zhang*,‡

Crystallography Research Program and Protein Studies Program, Oklahoma Medical Research Foundation, 825 NE 13th Street, Oklahoma City, Oklahoma 73104, and Department of Biochemistry and Molecular Biology, University of Oklahoma Health Sciences Center, 940 Stanton L. Young Street, Oklahoma City, Oklahoma 73104

Received August 5, 2003; Revised Manuscript Received September 19, 2003

ABSTRACT: GGA proteins regulate clathrin-coated vesicle trafficking by interacting with multiple proteins during vesicle assembly. As part of this process, the GAT domain of GGA is known to interact with both ARF and Rabaptin-5. Particularly, the GAT domains of GGA1 and -2, but not of GGA3, specifically bind with a coiled-coil region of Rabaptin-5. Rabaptin-5 interacts with Rab5 and is an essential component of the fusion machinery for targeting endocytic vesicles to early endosomes. The recently determined crystal structure of the GGA1 GAT domain has provided insights into its interactions with partner proteins. Here, we describe mutagenesis studies on the GAT−Rabaptin-5 interaction. The results demonstrate that a hydrophobic surface patch on the C-terminal three-helix bundle motif of the GAT domain is directly involved in Rabaptin-5 binding. A GGA3-like mutation, N284S, in this Rabaptin-5 binding patch of GGA1 led to a reduced level of Rabaptin-5 binding. Furthermore, a reversed mutation, S293N, in GGA3 partially establishes Rabaptin-5 binding ability in its GAT domain. These results provide a structural explanation for the binding affinity difference among GGA proteins. The current results also suggest that the binding of GAT to Rabaptin-5 is independent of its interaction with ARF.

Clathrin-coated vesicles (CCV)[1] represent a major type of vesicular carrier that moves between intracellular compartments as well as plasma membrane for the transport of both materials and cellular information (*1*). It has recently become clear that a family of GGA (Golgi-localized, γ-ear-containing, ARF binding) proteins play important roles in the CCV trafficking between *trans*-Golgi network (TGN) and endosome compartments, including cargo selection and recruitment of clathrin and accessory proteins to the budding site (*2*−*5*). GGA proteins are monomeric in solution and present in a variety of organisms (*2*−*8*). There are three GGA isoforms in humans (GGA1−3), each composed of four distinct domains. From the N- to C-terminus, the domains are VHS (VPS27, Hrs, and STAM), GAT (GGA and TOM1 homologous), hinge region, and GAE (γ-adaptin ear homologous). Important functions have been assigned to each of these domains (*3*, *6*, *9*, *10*). In particular, the GAT domain has been identified as the structural entity that interacts with the membrane-bound form of ARF (ADP ribosylation factor), a GTPase molecular switch initiating CCV assembly (*11*). The GAE domain has been shown to contain sites for interaction with many proteins, including Rabaptin-5, the ear domain of the γ-adaptin subunit of the AP-1 complex, and γ-synergin (*3*, *6*). Recently, the GAT domain has also been found to interact with Rabaptin-5, thus demonstrating a divalent interaction between GGA and Rabaptin-5 (*12*).

Rabaptin-5, an 862-residue protein, is an effector of Rab5 which functions as a molecular switch in the fusion of endocytic vesicles to early endosome (*13*, *14*). The involvement of Rabaptin-5 in this process is an essential and rate-limiting step (*15*). It is present mainly in the cytosol, but a small pool of this protein is also found at the cell membrane (*16*). Structurally, Rabaptin-5 appears to contain multiple coiled-coil regions, each of which is capable of forming homodimers *in vitro* (*15*) and may mediate *in vivo* dimerization (*17*). It is shown that an isolated Rabaptin-5 region of residues 551−661 can bind with the GAT domain of GGA1 and -2 (*12*), although the functional significance of this interaction is currently uncertain. Besides GGA, Rabaptin-5 interacts directly with the ear domain of the γ-adaptin subunit of the AP-1 adaptor complex (*18*), which is a major component of the CCV coating complex at TGN. Rabaptin-5 is also found to function in the endosome recycling pathway through its interaction with Rab4 (*17*).

The function of Rab5 is to ensure the correct directionality of vesicle trafficking and fusion to target compartments through interactions with downstream effectors (*19*). Like

† This work was supported in part by NIH Grant AG18933 and a Pioneer Award from the Alzheimer's Association to J.T., and an NSF CAREER Award to G.L.

* To whom correspondence should be addressed: Oklahoma Medical Research Foundation, 825 NE 13th St., Oklahoma City, OK 73104. E-mail: zhangc@omrf.ouhsc.edu. Fax: (405) 271-7953.

‡ Crystallography Research Program, Oklahoma Medical Research Foundation.

§ Protein Studies Program, Oklahoma Medical Research Foundation.

|| University of Oklahoma Health Sciences Center.

[1] Abbreviations: ARF, ADP-ribosylation factor; CBB, Coomassie brilliant blue; CCV, clathrin-coated vesicles; GAP, GTPase activating protein; GAT, GGA and TOM1 domain; GEF, guanidine nucleotide exchange factor; GGA, Golgi-localized, γ-ear-containing, ARF binding protein; GTP[S], guanosine 5′-*O*-(3-thiotriphosphate); HRP, horseradish peroxidase; TGN, trans-Golgi network.

10.1021/bi035392b CCC: $25.00
Published on Web 11/05/2003

ARF and other GTPase switches, Rab5 alternates between the active GTP-bound and inactive GDP-bound forms. The active form is usually promoted by a guanine nucleotide exchange factor (GEF), while the inactive form results from GTP hydrolysis promoted by a GTPase activating protein (GAP). The conformational difference between the active and inactive forms of the molecular switch is sensed by downstream effectors, and the information is propagated and sometimes amplified along the trafficking pathway. As an effector, Rabaptin-5 interacts with GTP-Rab5 through a highly conserved C-terminal domain (residues 789−862) (*17*). In addition, Rabaptin-5 uses an upstream sequence to form a tight complex in the cytosol with a Rab5-specific GEF, Rabex5 (*20*), comprising a key component of the fusion machinery. Interestingly, the hydrolysis of Rabaptin-5 by an apoptotic protease (*21*) results in the loss of membrane fusion activity. This observation opens the possibility of involvement of Rabaptin-5 in the regulation of endosome fusion during apoptosis.

The crystal structure of the GGA1 GAT domain, recently determined by us and others (*22*−*25*), shows that it contains four helices in an elongated overall shape. The longest helix participates in two structural motifs: an N-terminal helix−loop−helix motif and a C-terminal three-helix bundle. The N-terminal motif contains a hydrophobic surface patch, which is found to directly interact with ARF in a complex crystal structure (*24*). The elongated structure and its surface characteristics are consistent with the multiple functional roles for the GAT domain. To gain insight into the structural basis underlying the function of GAT−Rabaptin-5 interaction, we carried out a structural modification study on GAT, using point mutations and truncation variants. The results show that the three-helix bundle region of the GAT domain is intimately involved in Rabaptin-5 binding. Specifically, the interactions cluster in a hydrophobic patch located within the groove region between helices A3 and A4 of GAT. A GGA1- and -2-specific Rabaptin-5 binding determinant is identified within this patch.

EXPERIMENTAL PROCEDURES

Protein Expression and Purification. The constructs of the glutathione *S*-transferase (GST)−GAT (residues 141−326 of human GGA1) fusion and its three-helix bundle version (residues 210−326) have been described previously (*22*). For the expression of truncated GAT, $GGA1^{170-302}$, cDNA corresponding to this region was amplified with polymerase chain reaction and subcloned into the plasmid pGEX6P1 (Amersham Biosciences, Piscataway, NJ) to be expressed as a GST fusion protein. Point mutations were introduced into the GST−$GGA1^{141-326}$ parent construct in a pGEX6P1 plasmid, verified by sequencing and expressed in *Escherichia coli* strain BL21(DE3). Recombinant proteins from cell lysates were purified by affinity chromatography using a glutathione (GSH)−Sepharose 4B column (Amersham Biosciences) followed by Resource-Q ion exchange chromatography (Amersham Biosciences), dialyzed against 10 mM Tris-HCl (pH 8.5) and 0.1% (v/v) β-mercaptoethanol, and stored on ice. The protein concentration was calculated on the basis of the extinction coefficients ($\epsilon_{280} = 44\,000$ AU/M for GST−$GGA1^{141-326}$, GST−$GGA1^{170-302}$, and GST−$GGA1^{210-326}$ constructs) estimated from the amino acid sequence using the computer software Vector NTI (InforMax, Inc., Frederick, MD). In circular dichroism (CD) spectroscopic analysis, selected GAT mutants were subjected to a 190−300 nm wavelength scan using a J-715 spectropolarimeter (Jasco Inc., Easton, MD) to confirm their correct secondary structure contents. GST fusion proteins of the GAT domains of wild-type GGA2 (residues 157−342) and GGA3 (residues 147−313) and two variants with S293N (i.e., Ser293 to Asn) and S293D substitutions in the GST−$GGA3^{147-313}$ parent construct were expressed and purified in a similar manner.

To express the recombinant human Rabaptin-5 fragment (residues 551−862), Rabaptin-5 cDNA corresponding to this region was subcloned into the pET15b vector (Novagen, Madison, WI) and expressed in *E. coli* strain BL21(DE3). The recombinant His tag fusion protein was purified with affinity chromatography using the Hi-trap chelating column (Amersham Biosciences) charged with Ni^{2+}, and eluted with a buffer containing 0.2 M imidazole. This material was further purified using Resource-Q ion exchange chromatography, and a peak eluting at ∼250 mM NaCl was dialyzed against 10 mM Tris-HCl (pH 8.0) and 0.1% (v/v) β-mercaptoethanol and stored on ice. The protein concentration was determined using the Bradford protein assay (Bio-Rad Laboratories, Hercules, CA). A shorter construct encoding Rabaptin-5 residues 551−661 was subcloned into plasmid pET11a, and overexpressed as inclusion bodies. The refolding and purification for this protein were carried out using essentially the same procedure described previously (*26*). While Rabaptin-$5^{551-661}$ did not show oligomerization, Rabaptin-$5^{551-862}$ exhibited a strong tendency to form oligomers under a nonreduced condition in a native gel filtration experiment, presumably caused by two free cysteine residues (718 and 734) in the latter construct. In the presence of 0.2% β-mercaptoethanol, however, most of the recombinant Rabaptin-$5^{551-862}$ molecules remained a lower-molecular weight form [presumably dimers (*17*)]. The construct of the GTPase domain of human Rab5a encoding residues 13−184 and its purification have been discussed previously (*27*).

GST-Mediated Pull-Down Assay for Studying GAT−Rabaptin-5 Interaction. An aliquot containing ∼30 μg of a GST−GAT variant fusion protein was incubated for 30 min at 22 °C with 20 μL of a 50% slurry of GSH−Sepharose 4B beads in a final volume of 500 μL of binding buffer containing 1× PBS [phosphate-buffered saline (pH 7.4)], 0.2% (v/v) Triton X-100, and 0.2% (v/v) β-mercaptoethanol, supplemented with a protease inhibitor cocktail (Roche Diagnostics, Mannheim, Germany). Beads containing immobilized GST fusion protein were washed three times by resuspension in 1 mL of 1× PBS and centrifugation (3 min at 2000*g*). Washed beads were incubated for 2 h at 4 °C with 30 μg of recombinant Rabaptin-$5^{551-862}$ in 1 mL of binding buffer, washed three times each with 1 mL of binding buffer, resuspended in 30 μL of 2× SDS sample buffer, incubated for 10 min at 90 °C, and centrifuged to recover proteins of the complex from the supernatant. The sample was subjected to 12.5% SDS−PAGE analysis and visualized with Coomassie brilliant blue (CBB) stain.

Assay of ARF−GAT Binding. A pCDNA3 expression vector containing cDNA of the full-length human $ARF1^{Q71L}$ mutant (residues 1−181) was transfected into HeLa cells for transient expression of ARF1 using the Lipofectamin 2000 transfection kit (Invitrogen, Carlsbad, CA). The transfected

cells were grown in a T-25 culture flask for 36 h, resuspended in buffer A containing 1× PBS, 1 mM EDTA, 1 mM $MgCl_2$, 1 mM dithiothreitol (DTT), 1% (v/v) NP40 detergent, and protease inhibitor cocktail, and lysed by repeated ejection of the cells through a 21 gauge needle. The supernatant of the homogenate, first collected from low-speed centrifugation for 10 min at 4 °C and then at 120000*g* for 1 h at 4 °C, was used for the binding assays. An aliquot of supernatant (60 μL containing ~50 μg of total cell lysate proteins) was preincubated in buffer A with 30 μM GTP analogue guanosine 5′-*O*-(3-thiotriphosphate) (GTP[S], Roche, Indianapolis, IN) for 30 min and then with 10 μg of the GST−GGA1$^{141-326}$ fusion protein (prebound to 25 μL of a 50% slurry of GSH−Sepharose 4B beads) in the presence of varied concentrations of Rabaptin-5$^{551-862}$ (final volume of 170 μL) for 1 h at 22 °C with gentle shaking. The beads were washed three times with 500 μL of buffer A and placed in 25 μL of 2× SDS sample buffer at boiling temperature. The eluted protein was subjected to 10% SDS−PAGE and blotted onto PVDF membrane (Millipore Co., Bedford, MA). The blot was incubated sequentially with monoclonal mouse anti-ARF antibody (Affinity Bioreagents, Golden, CO) and then peroxidase-conjugated anti-mouse IgG and detected on film using Renaissance Chemiluminescence Reagent plus (Amersham Biosciences). The presence of Rabaptin-5 in the complex was confirmed by CBB stain.

Biomolecular Interaction Analysis Using Surface Plasmon Resonance. Affinity binding constants for association of GGA1 GAT with Rabaptin-5 fragments were quantitatively determined by surface plasmon resonance (SPR) using a BIACORE 3000 biosensor (BIACORE Inc.). Recombinant GGA1$^{141-326}$ with the N-terminal GST fusion protein cleaved was prepared at a concentration of 5 μg/mL in 10 mM sodium acetate (pH 5.0) and immobilized onto the sensor chip surface of a carboxymethylated dextran matrix in random orientations, primarily through reactions between carboxyl moieties of the dextran and amino residues on the protein surface. Sequential injections were applied to achieve an average surface density of 500 RU (response unit). Analyses were performed in a running buffer of 10 mM HEPES (pH 7.2), 150 mM NaCl, 0.1 mM DTT, and 0.005% (v/v) P-20 surfactant at 25 °C. Rabaptin-5$^{551-862}$ and Rabaptin-5$^{551-661}$ in varied concentrations (0.05−2.5 mM) were injected over the sensor surface for 3 min, at 30 μL/min, followed by a 3 min buffer-only dissociation period. Interactions were recorded in the form of sensorgrams with nonspecific refraction subtracted automatically and concurrently. After each cycle, the sensor surface was regenerated by injecting 5 μL of 2 M $MgCl_2$ and 1 mM DTT followed by a 2 min equilibration in the running buffer. First the dissociation rate constant (k_{off}) and then the association rate constant (k_{on}) were calculated using homogeneous kinetics for dissociation and association type-1 models through BIAevaluation software (version 3.1). Apparent equilibrium dissociation constants were calculated using the equation $K_D = k_{off}/k_{on}$, based on a model on average of one GAT binding site per Rabaptin-5 monomer.

Horseradish Peroxidase Uptake Assay. The cDNA of the GGA1 GAT domain (residues 147−314 of GGA1) was subcloned into the unique *Xba*I site of the double subgenomic Sindbis virus vector Toto1000:3′2J, and the resulting construct was used to generate recombinant viruses capable of expressing the target protein as described previously (*28*, *29*). Confluent BHK-21 (baby hamster kidney) cell monolayers were grown in α-minimal essential medium (α-MEM) containing 5% fetal bovine serum in 35 mm culture dishes. The cells were infected with either an empty-vector virus as a negative control or the recombinant virus expressing GAT and incubated at 37 °C in a tissue culture incubator with 5% CO_2 for 4 h. Horseradish peroxidase (HRP) uptake was initiated by replacing the medium with serum-free α-MEM containing 5 mg/mL HRP and 1% bovine serum albumin, followed by a 30 min incubation at 37 °C. The internalized HRP activity was then analyzed as described previously (*28*). The GAT domain contained an engineered Myc epitope fused to its N-terminus, which allowed us to confirm the overexpression of the GAT domain in the cell by Western blot analysis with an anti-Myc antibody (Sigma, St. Louis, MO). Another GAT construct without the Myc tag was also constructed and analyzed, and the results were essentially the same.

RESULTS

Rabaptin-5 Binds to the C-Terminal Three-Helix Bundle of the GAT Domain. The GGA1 GAT domain contains two distinct structural regions: an N-terminal helix−loop−helix motif and a C-terminal three-helix bundle motif. We previously demonstrated that a GGA1 fragment, GGA1$^{210-326}$ (Figure 1A), which encompasses the three-helix bundle and a 24-residue extension at the C-terminus, binds to a Rabaptin-5 C-terminal fragment, Rabaptin-5$^{551-862}$, with an affinity comparable to that of the construct containing the full-length GAT domain, GGA1$^{141-326}$ (*22*). In the current study, we first confirmed a previous observation seen in a yeast two-hybrid assay (*12*); i.e., Rabaptin-5 exhibits different binding affinities for the three GAT domains from GGA1 to GGA3. In our GST-mediated pull-down assay of recombinant GAT and Rabaptin-5 proteins, GGA3 GAT did not bind with Rabaptin-5$^{551-862}$, while GGA1 and -2 GAT domains exhibited roughly 1:1 binding (Figure 2A). To further discern the interacting region, we constructed another GAT fragment, GGA1$^{170-302}$, which excludes the terminal mobile regions in the crystal structure. In a pull-down experiment, we observed that the immobilized GST fusions of both GGA1$^{170-302}$ and GGA1$^{210-326}$ could effectively retrieve Rabaptin-5 (Figure 2B), suggesting that the binding affinity resides in the overlapped region of the two constructs, i.e., residues 210−302 of GGA1.

Two Rabaptin-5 fragments were prepared and compared for their ability to interact with full-length GGA1 GAT. Rabaptin-5$^{551-661}$ had been shown to interact with the GGA1 and -2 GAT domains (*12*), while a longer fragment, Rabaptin-5$^{551-862}$, extended into the C-terminal Rab5 binding domain. In a surface plasma resonance experiment, the recombinant protein of the shorter construct, Rabaptin-5$^{551-661}$, exhibited ~5-fold stronger binding than the longer one, mainly due to a faster on-rate (Table 1). It suggests that, under these experimental conditions, the extra C-terminal segment in the longer construct hinders binding to the GAT domain by making it somewhat less accessible.

Delineation of the Structural Determinants of Rabaptin-5−GAT Interaction. On the basis of our recently determined crystal structure of the GGA1 GAT domain, we carried out

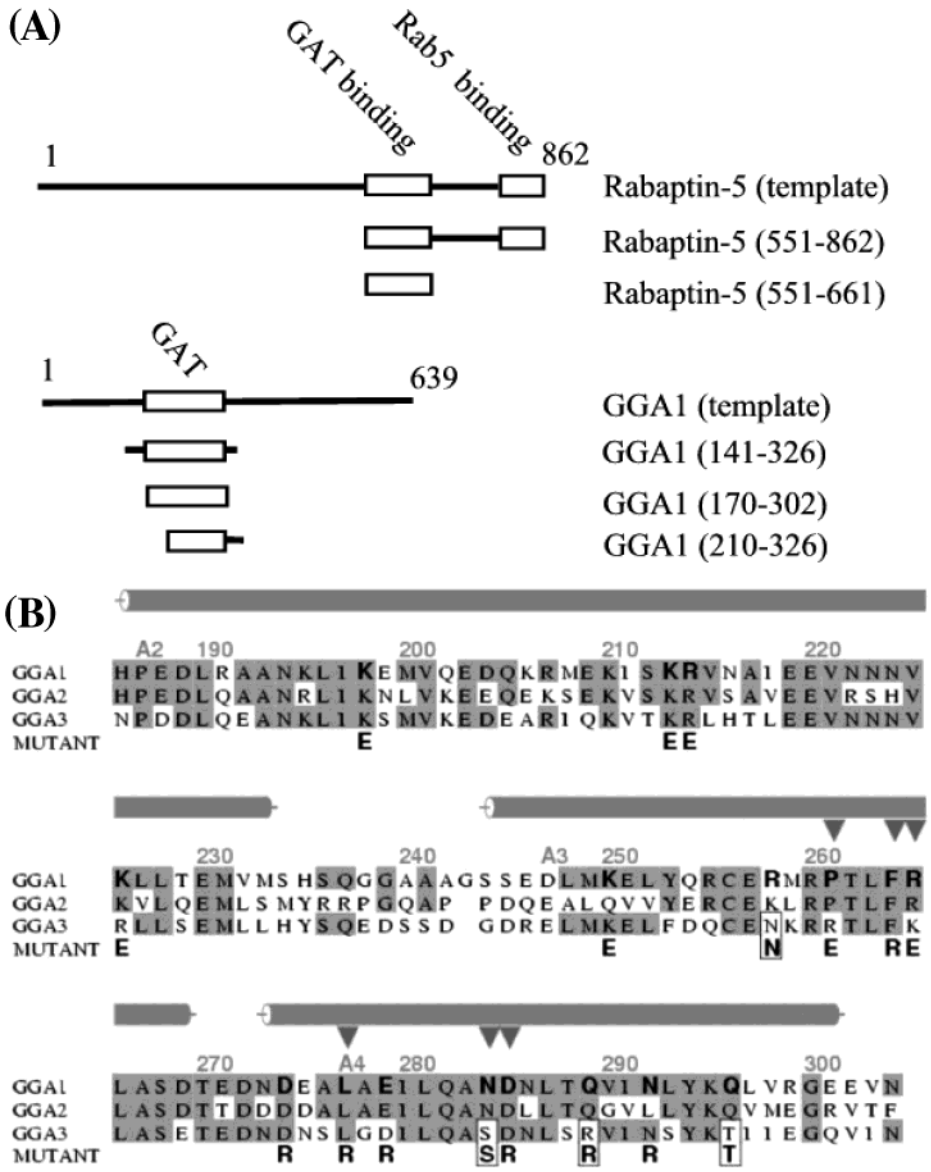

FIGURE 1: Constructs and mutations. (A) Multiple truncation constructs were made from Rabaptin-5 and GGA1. Relevant functional motifs or domains are boxed and labeled. (B) The amino acid sequence of the three-helix bundle region of the GGA1 GAT domain, including the full length of helix A2, is aligned with those of GGA2 and GGA3, followed by point mutations which were introduced into the GGA1$^{141-326}$ background. GGA1 sequence numbers and positions of helices A2−A4 (*22*) are marked on top of the sequences. GGA3-like mutations are boxed. Positions showing mutations affecting Rabaptin-5 binding are marked with triangles.

mutagenesis studies on GGA1 GAT to identify residues that are important for its interaction with Rabaptin-5. A total of 18 individual point mutations were introduced at 17 positions in GGA1 GAT (Figure 1B, plus P261R). Most of them were designed to invert or introduce electric charges to maximize the mutational effect on the GAT−Rabaptin-5 interaction. Five mutations adopted the residues from human GGA3 (boxes in Figure 1B, plus P261R) since it has been shown not to bind Rabaptin-5 (*12*) (see Figure 2A). The remaining mutations were selected to cover a wide surface area of the three-helix bundle motif. Pull-down experiments showed that mutants P261E, F264R, R265E, L277R, N284S, and D285R of GGA1 GAT exhibited drastically reduced affinity for Rabaptin-5 (Figure 3A). The possibility that the lack of binding was due to incorrect folding is unlikely as the CD spectra of these mutant proteins were similar to that of the wild-type GAT (data not shown). Examination of the location of these six affected residues in the crystal structure of GAT revealed that they clustered around a hydrophobic patch on the surface of helices A3 and A4 (Figure 3B,C). These results suggest that the hydrophobic patch of GGA1 GAT, including the six residues, plays an important role in the interaction with Rabaptin-5. Furthermore, of the GGA3-like substitution mutants that we selected in this experiment, two were located in this Rabaptin-5 binding patch: the N284S substitution exhibited a reduced affinity, while the P261R retained its binding ability. Interestingly, the P261E substitution at the latter position abrogated the binding.

A GGA1-like Mutation Establishes Rabaptin-5 Binding Ability in the GGA3 GAT Domain. While the wild-type GGA3 GAT domain lacks Rabaptin-5 binding ability (see Figure 2A), the GGA3-like GGA1 GAT mutant, N284S, described previously, weakened the binding ability of GGA1. A question naturally follows. Can the Rabaptin-5 binding ability be established in GGA3 by introducing a GGA1-like mutation? To address this question, we introduced a point

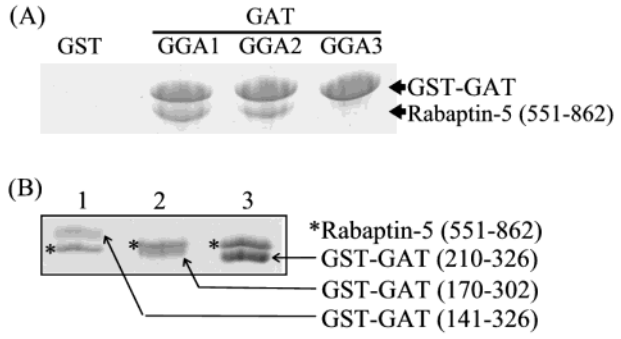

FIGURE 2: GAT−Rabaptin-5 interactions. (A) Interactions of the GAT domain from GGA1−GGA3 and the Rabaptin-5 C-terminal fragment were assayed with a GST-mediated pull-down experiment. (B) Pull-down assays for interactions between the GGA1 GAT truncation variants and Rabaptin-$5^{551-862}$. Fusion proteins of GST−GAT variants, i.e., $GGA1^{141-326}$ (lane 1), $GGA1^{170-302}$ (lane 2), and $GGA1^{210-326}$ (lane 3), were prebound to GSH−Sepharose beads and incubated with recombinant Rabaptin-$5^{551-862}$. The material bound to the beads was subjected to SDS−PAGE and CBB staining.

Table 1: Affinity Data for Rabaptin-5 Variants Binding to GAT[a]

	k_{on} ($\times 10^5$ M^{-1} s^{-1})	k_{off} ($\times 10^{-3}$ s^{-1})	K_D (nM)
$GGA1^{141-326}$, Rabaptin-$5^{551-661}$	4.4 ± 0.2	8.8 ± 0.2	20 ± 1
$GGA1^{141-326}$, Rabaptin-$5^{551-862}$	0.63 ± 0.2	6.1 ± 0.3	97 ± 36

[a] Data were measured with a BIACORE biosensor. Rabaptin-5 variants, each at 10 varied concentrations, were injected over the sensor surface bound with GAT, and the binding interactions were recorded in the form of sensorgrams, from which association and dissociation constants were determined on the basis of global fittings. Standard error values were estimated on the basis of the results from two independent experiments, each of which contains duplicated measurements.

mutation, S293N, into the GGA3 GAT domain and performed a GST-mediated pull-down experiment to assay Rabaptin-5 binding. Sequence alignment indicates that Ser293 of GGA3 corresponds to Asn284 of GGA1 (see Figure 1B); therefore, the S293N mutant of GGA3 was selected to establish the binding ability. A second mutation, S293D, which is structurally similar but chemically different from the previous one, was also made in the same background construct as a control. As shown in Figure 3D, the results demonstrated that the GGA1-like S293N mutation, but not its homologous mutant S293D, was able to partially establish the Rabaptin-5 binding ability in the GGA3 GAT domain. The difference between the two mutants suggests that a specific interaction of position 293 in GGA3 with Rabaptin-5 is required for the binding. On the other hand, the binding is noticeably weaker than that of the GGA1 GAT domain, implying that contributions to the binding from other GGA1 sites are absent in GGA3.

Binding of Rabaptin-5 to GAT Is Independent of the GAT−ARF Interaction. Since both ARF and Rabaptin-5 bind to the GGA1 GAT domain, we addressed the question of whether these two interactions were interdependent. To test such a possibility, we carried out a GST-mediated pull-down experiment to study effects of Rabaptin-5 on the ARF−GAT interaction. Cell lysate from HeLa cells containing a constitutively activated ARF1 mutant ($ARF1^{Q71L}$) was allowed to bind the GST−$GGA1^{141-326}$ construct in the presence of varying amounts of Rabaptin-$5^{551-862}$. We observed no detectable differences in ARF binding at any concentration of Rabaptin-$5^{551-862}$ (Figure 4), suggesting that ARF1 and Rabaptin-$5^{551-862}$ bind to GAT independently.

Overexpression of the GGA1 GAT Domain in Mammalian Cells Has No Effect on Endocytosis. Since Rab5−Rabaptin-5 interaction is crucial for endocytosis, we addressed the possibility that overexpression of GGA GAT could cause a dominant-negative inhibition of Rab5−Rabaptin-5 interaction and thus abrogate endocytosis; such interference could implicate a functional role for the Rabaptin-5 interaction with GAT-containing proteins. The endocytic activity of BHK cells overexpressing the GGA1 GAT domain was monitored following HRP uptake. We observed that the activity of HRP internalization was essentially unaffected by GAT overexpression as compared to a negative control of an empty vector (data not shown). For comparison, with an expression level similar to that of the GAT domain, a dominant-negative Rab5 mutant reduced the rate of HRP uptake by more than 80% (*30*). These results indicate that the endogenous Rab5−Rabaptin-5 interaction is not disrupted in these cells by the overexpressed GGA1 GAT domain. Consistent with biochemical data showing that Rab5 and GAT bind to different sites on Rabaptin-5 (*12*, *17*), it is possible that Rab5 and a GAT-containing protein may simultaneously bind to Rabaptin-5 and form a ternary complex that remains functional in endocytosis.

DISCUSSION

The cellular function of GGA proteins in vesicular trafficking is endowed largely by its four domains interacting with multiple protein partners. The GAT domain, second from the GGA1 N-terminus, is known to interact with two proteins, ARF and Rabaptin-5. Interaction of GAT with ARF (*9*) defines the vesicle-assembling site on the membrane and facilitates subsequent interactions with other proteins in the assembly complex (*4*). The structural component of GAT attributed to this interaction is the highly conserved N-terminal helix−loop−helix motif (*22*−*24*). Interaction of GAT with Rabaptin-5, particularly with regard to GGA1 and GGA2, is presumably a part of the mechanism for delivery of transport vesicles to target compartments (*12*).

Data from the current study suggest that a hydrophobic patch on the surface of the three-helix bundle motif of GGA1 GAT is intimately involved in its interaction with Rabaptin-5 (see Figure 3). This patch includes residues Pro261, Phe264, Leu277, and Leu281. Mutations at residues Arg265, Asn284, and Asp285 also diminished the level of Rabaptin-5 binding, indicating that these and perhaps other hydrophilic residues bordering the hydrophobic patch may also be involved in the binding. The postulated Rabaptin-5 binding surface is ~15 Å across, judging from the crystal structure of GGA1 GAT (*22*). Meanwhile, the GAT binding region of Rabaptin-5 (residues 551−661) is predicted to be a parallel coiled coil (*17*). Thus, its interaction with GAT likely involves helix surfaces from the two proteins, for example, through helix bundling. Since the molar ratio of GAT to Rabaptin-5 is likely to be 1:1 (see Figure 2A), two GAT domains may symmetrically bind to the Rabaptin-5 coiled-coil dimer (*17*). The putative Rabaptin-5 and ARF binding (*22*−*24*) sites are located in the two motifs of the GAT structure with a distance of >35 Å (from C_α^{178} to C_α^{281} of GGA1) and face opposite directions (see Figure 3B) (*24*). This distance and orientation

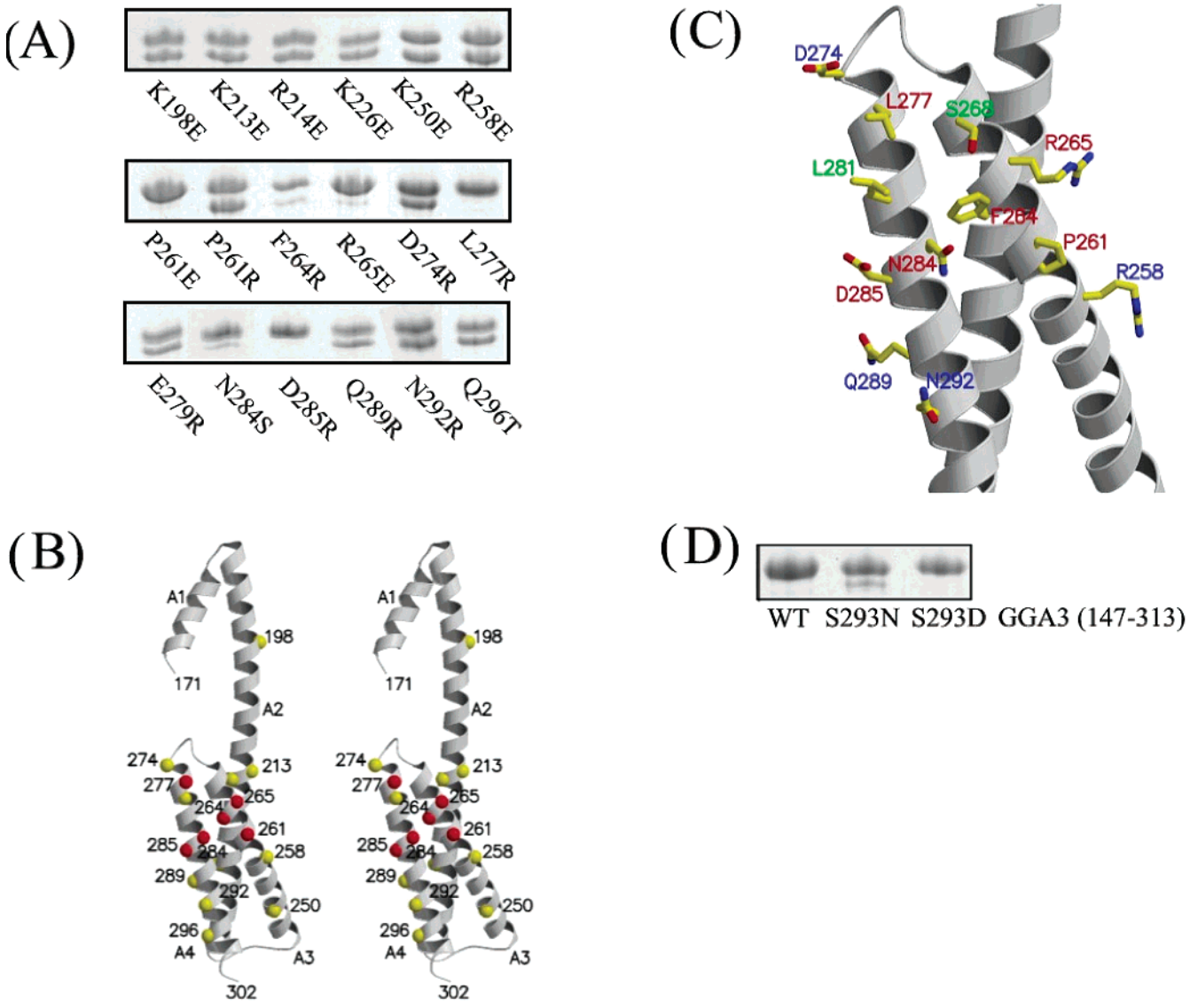

FIGURE 3: Effects of point mutations of GGA1 GAT on Rabaptin-5 binding. (A) Pull-down assays for interactions between the GGA1 GAT mutants and Rabaptin-$5^{551-862}$. Recombinant fusion proteins of GST−$GGA1^{141-326}$ variants were prebound to GSH−Sepharose beads and incubated with recombinant Rabaptin-$5^{551-862}$. The material bound to the beads was subjected to SDS−PAGE and CBB staining. The top band is GST−$GGA1^{141-326}$ (48 kDa), and the bottom band is Rabaptin-$5^{551-862}$ (36 kDa). The experiment was repeated multiple times, and the results were essentially the same. (B) Stereoview of the distribution of the point mutations in the three-dimensional structure of GAT. C_α atom positions of the point mutations are marked with spheres. Those affecting Rabaptin-5 binding are colored red; otherwise, they are colored yellow. (C) Structure of the putative Rabaptin-5 binding site of GAT. Residues known to be involved in the binding are labeled in red; those not involved are labeled in blue, and those unknown in binding are labeled in green. (D) Pull-down assays for interactions between the GGA3 GAT mutants and Rabaptin-$5^{551-862}$. Experimental details were the same as those for panel A, except GGA1 variants were replaced with $GGA3^{147-313}$ variants.

are consistent with our observation that ARF and the Rabaptin-5 C-terminal fragment bind to GAT independently (see Figure 4).

Rabaptin-5 has been shown to have different binding affinities for three human GGAs (Figure 2A) (*12*); the functional consequence of this difference, however, remains unclear. Although the three-helix bundle region of GAT is only moderately conserved among the three human GGAs, the degree of homology of the residues within the proposed Rabaptin-5 binding patch is significantly higher. One notable exception is found in the middle of helix A3, where Pro261 in GGA1 and -2 becomes an arginine residue in GGA3. This proline residue clearly contributes to a kink at the middle of helix A3 (residues 244−269) in the GGA1 structure (*22*−*25*). The reduction in the binding affinity of the P261E mutant indicates that a residue at this position is involved in the binding either via a direct contact with Rabaptin-5 or indirectly by changing the local conformation on the GAT side. The GGA3-like P261R mutation did not show a significant change in Rabaptin-5 binding, suggesting that this position is not responsible for the specificity that distinguishes between GGA1 and GGA3 in terms of their ability to bind Rabaptin-5. However, N284S, another GGA3-like mutation in the patch, showed a reduced level of Rabaptin-5 binding, thus providing a plausible explanation for the difference in the Rabaptin-5 binding specificity among the three GGAs. Such a possibility is further supported by a reversed mutation that changes Ser293 of GGA3 to the corresponding GGA1 residue, Asn, and partially establishes Rabaptin-5 binding ability in the otherwise incompetent

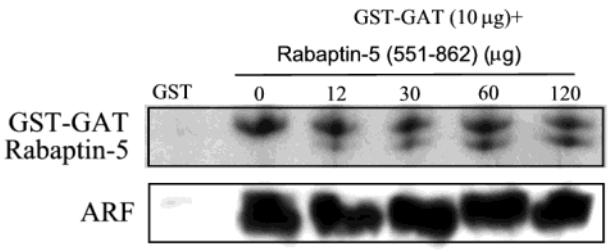

FIGURE 4: GAT−Rabaptin-5 binding does not disrupt the GAT−ARF interaction. GST alone (negative control) or the GST−GGA1$^{141-326}$ fusion protein (10 μg) was preincubated with GSH−Sepharose beads and cell lysate containing ARF1^{Q71L} in the presence of different concentrations of Rabaptin-5$^{551-862}$ (0−120 μg). The material bound to the beads was subjected to SDS−PAGE and CBB staining (for GST−GAT constructs and Rabaptin-5) or Western blotting (for ARF1). This pull-down assay shows no effect of Rabaptin-5 on the GAT−ARF interaction. The experiment was repeated multiple times, and the results were identical.

GGA3 GAT domain (see Figure 3D). The current mutagenesis results also allow an examination of Rabaptin-5 binding potential in proteins with domains homologous to GAT. For example, TOM1-like proteins (*4*) are moderately homologous with the C-terminal three-helix bundle region (*22*) of GGA GAT but are devoid of the ARF binding helix−loop−helix motif and, thus, do not bind to the Golgi membrane (*31*). The residues corresponding to the Rabaptin-5 binding hydrophobic patch of the GGA GAT are not conserved in TOM1. The N-terminal domain of syntaxin proteins shares a similar folding topology with the GGA1 GAT domain (*25*), although the level of homology is meager at the primary sequence level. For example, in syntaxin-6 (PDB entry 1lfv), no hydrophobic patch equivalent is observed in its three-helix bundle. Therefore, it is unlikely that these proteins would bind Rabaptin-5 through a mechanism similar to that used by a GGA GAT.

What could be the functional significance of the Rabaptin-5−GGA interaction? Since Rabaptin-5 plays important roles in early endosome fusion (*15*), it is hypothesized that the GGA−Rabaptin-5 interaction enables fusion of TGN-derived vesicles with endosomes (*12*), allowing the unloading of cargos from the TGN to the endosomal system (*32*). The GGA proteins promote ARF-dependent recruitment of clathrin to the TGN through its hinge region C-terminal to the GAT domain (*31*). Binding of Rabaptin-5 to the GAT domain, on the other hand, leads to the dissociation of clathrin from the vesicle. In addition, *in vivo* overexpression of Rabaptin-5 shifts the localization of intracellular GGA1 and diverts the association of cargo to enlarged early endosomes (*12*). These observations suggest a possibility that GGA−Rabaptin-5 interaction promotes the endosome fusion process by shedding clathrin. Our current data suggest that Rabaptin-5 binding does not disrupt GGA−ARF interaction (see Figure 4). Thus, the dissociation of clathrin may not be a direct result of dissociation of GGA from ARF; instead, Rabaptin-5 may interfere with the GGA−clathrin binding through a stereo and/or electrostatic conflict.

ACKNOWLEDGMENT

We thank Drs. P. Mehta and K. Rodger for helping with the BIACORE and CD experiments and W. Radosevich for technical assistance. We are grateful to Dr. M. Robinson (University of Cambridge, Cambridge, England) for providing the cDNA of human GGAs, Dr. G. Grenningloh (University of Lausanne, Lausanne, Switzerland) for the Rabaptin-5 cDNA, and Dr. K. Nakayama (Kanazawa University, Kanazawa, Japan) for the ARF1 cDNA.

REFERENCES

1. Kirchhausen, T. (2000) Clathrin, *Annu. Rev. Biochem. 69*, 699−727.
2. Poussu, A., Lohi, O., and Lehto, V. P. (2000) Vear, a novel Golgi-associated protein with VHS and gamma-adaptin "ear" domains, *J. Biol. Chem. 275*, 7176−7183.
3. Hirst, J., Lui, W. W., Bright, N. A., Totty, N., Seaman, M. N., and Robinson, M. S. (2000) A family of proteins with gamma-adaptin and VHS domains that facilitate trafficking between the trans-Golgi network and the vacuole/lysosome, *J. Cell Biol. 149*, 67−80.
4. Dell'Angelica, E. C., Puertollano, R., Mullins, C., Aguilar, R. C., Vargas, J. D., Hartnell, L. M., and Bonifacino, J. S. (2000) GGAs: a family of ADP ribosylation factor-binding proteins related to adaptors and associated with the Golgi complex, *J. Cell Biol. 149*, 81−94.
5. Boman, A. L., Zhang, C., Zhu, X., and Kahn, R. A. (2000) A family of ADP-ribosylation factor effectors that can alter membrane transport through the trans-Golgi, *Mol. Biol. Cell 11*, 1241−1255.
6. Takatsu, H., Yoshino, K., and Nakayama, K. (2000) Adaptor gamma ear homology domain conserved in gamma-adaptin and GGA proteins that interact with gamma-synergin, *Biochem. Biophys. Res. Commun. 271*, 719−725.
7. Black, M. W., and Pelham, H. R. (2000) A selective transport route from Golgi to late endosomes that requires the yeast GGA proteins, *J. Cell Biol. 151*, 587−600.
8. Zhdankina, O., Strand, N. L., Redmond, J. M., and Boman, A. L. (2001) Yeast GGA proteins interact with GTP-bound Arf and facilitate transport through the Golgi, *Yeast 18*, 1−18.
9. Takatsu, H., Yoshino, K., Toda, K., and Nakayama, K. (2002) GGA proteins associate with Golgi membranes through interaction between their GGAH domains and ADP-ribosylation factors, *Biochem. J. 365*, 369−378.
10. Puertollano, R., Aguilar, R. C., Gorshkova, I., Crouch, R. J., and Bonifacino, J. S. (2001) Sorting of mannose 6-phosphate receptors mediated by the GGAs, *Science 292*, 1712−1716.
11. Moss, J., and Vaughan, M. (1998) Molecules in the ARF orbit, *J. Biol. Chem. 273*, 21431−21434.
12. Mattera, R., Arighi, C. N., Lodge, R., Zerial, M., and Bonifacino, J. S. (2003) Divalent interaction of the GGAs with the Rabaptin-5-Rabex-5 complex, *EMBO J. 22*, 78−88.
13. Bucci, C., Parton, R. G., Mather, I. H., Stunnenberg, H., Simons, K., Hoflack, B., and Zerial, M. (1992) The small GTPase Rab5 functions as a regulatory factor in the early endocytic pathway, *Cell 70*, 715−728.
14. Li, G. (1996) Rab5 GTPase and endocytosis, *Biocell 20*, 325−330.
15. Stenmark, H., Vitale, G., Ullrich, O., and Zerial, M. (1995) Rabaptin-5 is a direct effector of the small GTPase Rab5 in endocytic membrane fusion, *Cell 83*, 423−432.
16. Gournier, H., Stenmark, H., Rybin, V., Lippe, R., and Zerial, M. (1998) Two distinct effectors of the small GTPase Rab5 cooperate in endocytic membrane fusion, *EMBO J. 17*, 1930−1940.
17. Vitale, G., Rybin, V., Christoforidis, S., Thornqvist, P., McCaffrey, M., Stenmark, H., and Zerial, M. (1998) Distinct Rab-binding domains mediate the interaction of Rabaptin-5 with GTP-bound Rab4 and Rab5, *EMBO J. 17*, 1941−1951.
18. Shiba, Y., Takatsu, H., Shin, H. W., and Nakayama, K. (2002) γ-Adaptin interacts directly with Rabaptin-5 through its ear domain, *J. Biochem. 131*, 327−336.
19. Rubino, M., Miaczynska, M., Lippe, R., and Zerial, M. (2000) Selective membrane recruitment of EEA1 suggests a role in directional transport of clathrin-coated vesicles to early endosomes, *J. Biol. Chem. 275*, 3745−3748.
20. Horiuchi, H., Lippe, R., McBride, H. M., Rubino, M., Woodman, P., Stenmark, H., Rybin, V., Wilm, M., Ashman, K., Mann, M., and Zerial, M. (1997) A novel Rab5 GDP/GTP exchange factor complexed to Rabaptin-5 links nucleotide exchange to effector recruitment and function, *Cell 90*, 1149−1159.

21. Cosulich, S. C., Horiuchi, H., Zerial, M., Clarke, P. R., and Woodman, P. G. (1997) Cleavage of Rabaptin-5 blocks endosome fusion during apoptosis, *EMBO J. 16*, 6182−6191.
22. Zhu, G., Zhai, P., He, X., Terzyan, S., Zhang, R., Joachimiak, A., Tang, J., and Zhang, X. (2003) Crystal structure of the human GGA1 GAT domain, *Biochemistry 42*, 6392−6399.
23. Collins, B. M., Watson, P. J., and Owen, D. J. (2003) The structure of the GGA1-GAT domain reveals the molecular basis for ARF binding and membrane association of GGAs, *Dev. Cell 4*, 321−332.
24. Shiba, T., Kawasaki, M., Takatsu, H., Nogi, T., Matsugaki, N., Igarashi, N., Suzuki, M., Kato, R., Nakayama, K., and Wakatsuki, S. (2003) Molecular mechanism of membrane recruitment of GGA by ARF in lysosomal protein transport, *Nat. Struct. Biol. 10*, 386−393.
25. Suer, S., Misra, S., Saidi, L. F., and Hurley, J. H. (2003) Structure of the GAT domain of human GGA1: A syntaxin amino-terminal domain fold in an endosomal trafficking adaptor, *Proc. Natl. Acad. Sci. U.S.A. 100*, 4451−4456.
26. Zhai, P., Wakeham, N., Loy, J. A., and Zhang, X. C. (2003) Functional roles of streptokinase C-terminal flexible peptide in active site formation and substrate recognition in plasminogen activation, *Biochemistry 42*, 114−120.
27. Zhu, G., Liu, J., Terzyan, S., Zhai, P., Li, G., and Zhang, X. C. (2003) High-resolution crystal structures of human Rab5a and five mutants with substitutions in the catalytically important phosphate-binding loop, *J. Biol. Chem. 278*, 2452−2460.
28. Li, G., and Liang, Z. (2001) Phosphate-binding loop and Rab GTPase function: mutations at Ser29 and Ala30 of Rab5 lead to loss-of-function as well as gain-of-function phenotype, *Biochem. J. 355*, 681−689.
29. Frolov, I., Hoffman, T. A., Pragai, B. M., Dryga, S. A., Huang, H. V., Schlesinger, S., and Rice, C. M. (1996) Alphavirus-based expression vectors: strategies and applications, *Proc. Natl. Acad. Sci. U.S.A. 93*, 11371−11377.
30. Li, G., and Stahl, P. D. (1993) Structure−function relationship of the small GTPase Rab5, *J. Biol. Chem. 268*, 24475−24480.
31. Puertollano, R., Randazzo, P. A., Presley, J. F., Hartnell, L. M., and Bonifacino, J. S. (2001) The GGAs promote ARF-dependent recruitment of clathrin to the TGN, *Cell 105*, 93−102.
32. Puertollano, R., van der Wel, N. N., Greene, L. E., Eisenberg, E., Peters, P. J., and Bonifacino, J. S. (2003) Morphology and dynamics of clathrin/GGA1-coated carriers budding from the trans-Golgi network, *Mol. Biol. Cell 14*, 1545−1557.

BI035392B